

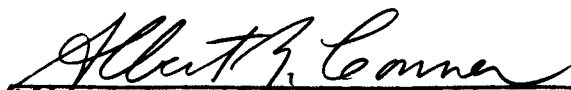
A STUDY OF THE MECHANISM OF CHEMICAL REACTIVITY
OF NITROGEN TETROXIDE WITH TITANIUM ALLOYS


THIRD QUARTERLY REPORT
January 1 through March 31, 1968

Sponsored by
The George C. Marshall Space Flight Center
National Aeronautics and Space Administration
Contract No. NAS8-21207
Control No. DCN 1-7-54-20173 (1F)

Submitted by
Research Center, Hercules Incorporated
Wilmington, Delaware 19899

April 15, 1968


Albert Z. Conner
Project Leader


Alan D. Craig, Manager
Explosives & Chemical Propulsion
Research Division

A STUDY OF THE MECHANISM OF CHEMICAL REACTIVITY
OF NITROGEN TETROXIDE WITH TITANIUM ALLOYS

Foreward

This is the third quarterly technical report prepared by the Research Center, Hercules Incorporated, under Contract No. NAS8-21207, Control No. DCN 1-7-54-20173 (1F) covering the period from January 1 through March 31, 1968. This report was prepared for the George C. Marshall Space Flight Center of the National Aeronautics and Space Administration. The work was administered under the technical direction of the Propulsion and Vehicle Engineering Laboratory, Materials Division of the George C. Marshall Space Flight Center with Mr. W. A. Riehl acting as project manager. The ninth monthly progress report has been integrated into this report. Scientific personnel currently participating in this program include:

Mr. A. Z. Conner, Project Leader

Dr. J. B. Arots	}	Corrosion Studies
Mr. A. H. Betley		

Dr. E. J. Forman, Analytical Coordination

Dr. G. A. Ward, NMR Studies

Mr. A. A. Orr, Spectrophotometer Studies

Mr. R. J. Friant, Mass Spectroscopic Studies

Dr. H. L. Young, Sample Preparation

Dr. J. F. G. Clarke, Jr., Gas Chromatography

Mr. Lawrence Haas, X-ray Emission

Mr. A. B. Peet, Optical Emission and Atomic Absorption
Spectroscopy

Mr. L. D. Missimer, Metals Analysis

ABSTRACT

Phase A - Development and Application of a Standard Stress Corrosion Cracking Test

The development of a satisfactory stress corrosion cracking (SCC) test for 6 Al 4V ELI titanium alloy exposed to liquid nitrogen tetroxide at 165°F. has successfully been completed. During the past three months, eleven SCC tests have been performed in which a total of 105 specimens have been exposed to Red Reactive (RR), Red Non-Reactive (RNR), Green 8 (G8), Green 4 (G4), and deoxygenated Red-Reactive N₂O₄.

The majority of the work during this quarter has been aimed at clarifying the roles of dissolved oxygen and N₂O₃ in the creation and inhibition of SCC. On the basis of this work, oxygen appears to be involved in the crack initiation and propagation mechanism. It has also been shown that as little as 500 ppm. NO added to N₂O₄ will prevent SCC. The critical level may be significantly lower. Additional work was done to assess the possible role of nitrous acid as a corrosion inhibitor but the results were not definitive.

Data are presented in this report concerning the effect of NO content on normal corrosion rates, the solubilities of various metals in liquid N₂O₄, and possible compositions of Red Non-Reactive N₂O₄.

A satisfactory method for the production of small amounts of dry, NO-free N₂O₄ has been devised and is in the process of scale-up in preparation for a series of critical add-back experiments involving H₂O, NO, and 100% HNO₃.

Phase B - Characterization of Propellant N_2O_4

During the past three months, development has essentially been completed on methods for the determination of traces of dissolved oxygen by gas chromatography and the determination of low levels of NO by visible spectroscopy.

The gas chromatographic procedure employs a unique helium-filled glove bag sampling system to eliminate contact of the samples and sample containers with atmospheric oxygen. Both liquid and gas phases can be analyzed. Analysis of the gas phase coupled with Henry's Law calculations can be used to estimate the dissolved oxygen content of the liquid phase below 1 ppm. Agreement between this procedure and direct analysis of the liquid phase is good above 10 ppm. O_2 , but some discrepancies remain to be resolved below this level.

Extension of the spectrophotometric method for the determination of NO down to <50 ppm. has been achieved. The analysis of known mixtures of NO in dried N_2O_4 has shown that protonated species do not contribute significant absorption at the measuring wave lengths, and the observed spectra represent only the sum of the N_2O_3 and N_2O_4 absorptions. The differential absorbance between 700 and 900 $m\mu$ has been found to be linearly dependent on NO concentration. The limit of detection of NO in N_2O_4 is approximately 15 ppm.

Considerable effort has been expended in comparing procedures for the determination of iron in N_2O_4 . This was primarily done to resolve discrepancies in results that indicated the possible presence of volatile Fe species in N_2O_4 . A number of different hydrolysis procedures, sample concentration steps, and analysis methods were

compared. Almost all of the combinations tested yielded consistent results, except for a bathophenanthroline colorometric method used at the Hercules, California, plant which gave high values. The vast majority of the data shows that the solubility of Fe in liquid N_2O_4 is less than 1 ppm., and that there is no significant amount of volatile iron species present.

Several attempts were made to resolve the proton resonance peaks that contribute to the "water" peak observed in the NMR spectrum of N_2O_4 . Solutions of N_2O_4 in $CHCl_3$ and CH_2Cl_2 were prepared and spectra obtained at -50° to $-60^\circ C$. No significant broadening of the "water" peak, indicative of a decrease in proton exchange rate, was observed. A few additional experiments with different solvents and lower temperatures will be performed, but the outlook is not promising.

TABLE OF CONTENTS

	<u>Page</u>
Abstract	2
Introduction	7
Phase A - Development and Application of a Standard Stress Corrosion Cracking Test	8
I. Stress Corrosion Cracking Tests	8
II. Test Cell Development	11
III. Corrosion Inhibition by Nitric Oxide	12
IV. Metal Solubility in N_2O_4	12
V. Production of Dry N_2O_4	13
VI. Red Non-Reactive N_2O_4	14
VII. Future Work	15
Phase B - Characterization of Propellant N_2O_4	18
I. Determination of Oxygen by Gas Chromatography	18
II. Determination of NO by Visible Spectroscopy	31
III. Determination of Dissolved Metals in N_2O_4	37
IV. Determination of Protonated Species by NMR	44

LIST OF FIGURES

	<u>Page</u>
Figure 1 - Relationship of Gas Versus Liquid Analysis	22
Figure 2 - Gas Chromatographic Sampling System	27
Figure 3 - Calibration Curve for Oxygen	30
Figure 4 - Absorption Spectra of Dried N_2O_4 Plus NO	34
Figure 5 - Replot of Spectra of Figure 4 from which the Contribution of Curve "O" has Been Subtracted	35
Figure 6 - Absorbence Versus NO Concentration	36

INTRODUCTION

The specific objectives of this program are as follows:

(1) To develop a standard stress corrosion test capable of assessing the corrosive nature of various types of dinitrogen tetroxide (N_2O_4) on 6 Al 4V titanium alloy specimens.

(2) To develop methods of analysis capable of detecting and determining significant differences between various types of N_2O_4 .

(3) To identify that constituent or component of N_2O_4 which enhances or induces stress corrosion in 6 Al 4V titanium alloy.

(4) To attempt to establish the possible presence of stress corrosion inhibitors in certain types of N_2O_4 and to determine the concentration levels that are critical regarding their inhibitory action.

This report describes the successful accomplishment of the first two specific objectives and the progress made during the past three months toward the achievement of the remaining goals.

Phase A. Development and Application of a Standard Stress Corrosion Cracking Test

I. Stress Corrosion Cracking Tests

The development of a satisfactory stress corrosion cracking (SCC) test for 6 Al 4 V ELI titanium alloy exposed to liquid nitrogen tetroxide at 165°F. has successfully been completed. During the past three months, eleven SCC tests have been performed in which a total of 105 specimens have been exposed to Red Reactive (RR), Red Non-Reactive (RNR), Green 8 (G8), Green 4 (G4), and deoxygenated Red Reactive N_2O_4 . The results of these tests are summarized in Table 1. The test has yielded highly consistent results as evidenced by the fact that, in a given set, all specimens either crack or do not crack.

Thus far it has been shown that no specimen cracks in normal production RR N_2O_4 to which 500 ppm. or more of nitric oxide has been added. Nitrogen tetroxide containing 500 ppm. NO is visually red and can be considered as an example of Red Non-Reactive N_2O_4 . The critical level of NO may be considerably less than 500 ppm. and remains to be established.

The possible role of nitrous acid as a corrosion inhibitor in liquid N_2O_4 systems was examined in a single test run (Run No. 13) in which the alloy specimens were given a pretreatment with aqueous HNO_2 before exposure to RR N_2O_4 . This pretreatment involved a 16-hour contact of the stressed (90%) U-bend specimens with aqueous HNO_2 that was prepared by the addition of N_2O_3 to NO-saturated distilled water. The specimens were dried before installation in the test cell. This pretreatment was ineffective since all specimens

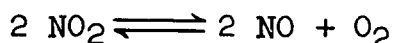
cracked in 67 hours at 163°F. However, because of the unfavorable kinetics of the decomposition of aqueous solutions of HNO_2 , the results of this test are not considered to be definitive. Additional experiments are planned. At present it is not certain that HNO_2 can exist at equilibrium in a N_2O_4 - N_2O_3 - H_2O system. However, if HNO_2 represents a significant percentage of the protonated species that are present, then it may be an important factor in corrosion inhibition.

The development of a satisfactory gas chromatographic method for the determination of traces of oxygen in N_2O_4 (see Phase B) has refocused attention on the role of O_2 in the SCC mechanism. In Run No. 9, it was observed that the oxygen level decreased during the test from 5.5 to 0.2 ppm. This reduction might have been due to a "gettering" action of the fresh titanium surfaces exposed during the cracking process. It thus appeared possible that oxygen might be involved in the crack initiation mechanism. In the SCC of stainless steel, there is some evidence that oxygen is necessary for the chloride cracking mechanism to function.

Three experiments were performed to investigate this phenomenon. In the first test (Run 10, Table 1), the usual ten U-bends were exposed at room temperature to RR N_2O_4 whose oxygen content had been reduced from 12.0 to 1.1 ppm. by sequential venting of the gas phase in the corrosion test cell during the first 12 hours of a 76-hour run. Only a limited number of cracks ($2\text{-}8/\text{cm}^2$) were observed, and all U-bends remained intact. Weight losses of the specimens were within experimental error, thus indicating a corrosion rate of <0.06 mils/year. The O_2 level did not decrease further during the test run.

The second experiment (Run 11, Table 1) employed regular RR N₂O₄ (20.1 ppm. O₂) at room temperature for 76 hours. All ten specimens developed numerous cracks (100-800/cm.²) during the test. The U-bends remained intact and the O₂ level decreased only slightly if at all (20.1 to 19.1 ppm.). Run 12 was made at 167°F. with RR N₂O₄ that had been deoxygenated from 20.1 to 0.08 ppm. The ten U-bends developed numerous cracks, all broke in two, and the O₂ appeared to remain at a very low level, 0.05 ppm.

These experiments suggest the involvement of oxygen in the crack initiation and propagation mechanisms, at least at room temperature. At the higher temperature, i.e., 165°F., the critical level of O₂ may be much lower than at room temperature. In addition, there is evidence(1) that the dissociation of NO₂:



actually begins at 60°C. There is also evidence(2) that the Henry's Law constants for O₂ and NO are considerably different at elevated temperatures. Thus it is conceivable that the level of dissolved O₂ could increase during an SCC test at 165°F.

The deoxygenation of RR N₂O₄ was approached in two ways. In four of the five experiments, O₂ was removed by outgassing at the atmospheric boiling point. This normally involved venting of the gas phase a number of times until the chromatographic analysis of either gas or liquid phase showed the desirable level of residual O₂. U-bend specimens were in place during this venting process, since the operation was carried out with a loaded test cell. Another procedure for removing oxygen from RR N₂O₄ is to add small amounts of G8 N₂O₄ or gaseous NO. Although accurate control of

these additions is difficult, it should be possible to produce an O_2 and NO-free material.

Minimum stress levels in 6 Al 4V ELI alloy for immunity to stress corrosion cracking in RR N_2O_4 have not been determined. Thus far, cracking has been observed (1) at the sheared edge formed during the cutting of flat blanks from the alloy sheet, (2) in prebends, (3) at identification stampings, and (4) with U-bends loaded to as little as 30% of the yield strength. Experiments to establish the stress threshold level could be fairly involved. Certainly machined, annealed, electropolished beam specimens would be needed and the state of stress under any of the test conditions would have to be checked by x-ray. A rough indication of the low "immune" stress level is provided by the 1/4-inch NC20 6Al 4V titanium bolts used to load the U-bends. The stress in these bolts is <5,000 psi. and the intermittent exposure time has been as high as 600 hours in RR N_2O_4 . However, since it is not known what relationships might exist between stress level, intermittent exposure, time of exposure, bolt configuration, thermal history, etc., it is doubtful if a bolt study would provide much insight into the problem.

The experiments conducted to date have shown that orientation of the specimens with respect to the rolling direction has no significant effect on the incidence of SCC under the test conditions.

II. Test Cell Development

The test cells used for the last 12 SCC tests have employed Teflon end-closures for the 3-inch diameter glass pipe cell body.

Minor leakage observed at the closure tubing protrusion and Swagelock valve fitting has been eliminated by changing from regular Teflon to glass-filled Teflon closures. The stiffer glass-filled Teflon seals better initially and exhibits much less creep during use. Type 304 stainless steel needle valves are still being used to seal off the cell during tests. The success of the test program indicates that the very small area of stainless steel exposed to N_2O_4 has no significant effect on the test results. Glass-filled Teflon needle valves have recently been made and will undergo thermal and pressure cycling tests. However, this work has assumed a low priority in the overall work program.

III. Corrosion Inhibition by Nitric Oxide

The inhibitory action of NO on the normal corrosion of the test alloy has been demonstrated by weight loss experiments at 162°-165°F. in which the corrosion rate has decreased with increasing NO content. In RR N_2O_4 the corrosion rate is $0.9^{+0.3}_{-0.2}$ mils/year. At the 500 ppm. NO level this decreases to $0.14^{+0.09}_{-0.05}$ mils/year, and at >4,000 ppm. NO becomes <0.06 mils/year. It should be noted that these experiments were carried out using N_2O_4 that contained 800-900 ppm. of protonated species calculated as water. Whether the presence of NO reduces corrosion in essentially anhydrous N_2O_4 remains to be shown.

IV. Metal Solubility in N_2O_4

Atomic absorption analysis data obtained during this program are summarized in Table 2. These data show that Fe, Al and Na have less than 1 ppm. solubility in RR N_2O_4 at room temperature. Titanium, under the same conditions, is considerably more soluble, i.e., up to 37 ppm. The solubility of vanadium is at least 9 ppm.

Nitrogen tetroxide containing 0.7-0.8% NO may permit a slightly higher solubility of Fe, i.e., up to 1.6 ppm. Solubilities of other metals in G8 N₂O₄ could not be established because of the very low corrosion rates observed during testing.

Insoluble material was isolated from the RR N₂O₄ used in Run 12. An acetone and alcohol wash of this gummy material left a white crystalline birefringent solid which contained Ti and Al. On a total solids basis, the proportions of Ti and Al match those of the alloy. Considerable Fe and Na were found but essentially no V. No attempt to identify the anion portion of the crystalline residue was made.

V. Production of Dry N₂O₄

Mechanism studies in this program may hinge on the availability of adequate test quantities of dry N₂O₄, preferably NO-free. The preparation of dry, NO-free N₂O₄ was attempted by a saturation procedure. Dry N₂ was bubbled through N₂O₄ at 20°C. and carried through a column filled with P₂O₅ coated beads. The gas was cooled and the condensate collected between 0 and -10°C. This condensate was found by NMR procedures to contain about 200 ppm. H₂O. This is too high a level for the proposed tests.

Additional experiments showed that much drier (<100 ppm. H₂O) material could be obtained by passing N₂O₄ vapors through a column of 3A molecular sieve and condensing the effluent. Nitric oxide (150 ppm.) was also formed in this operation but it could readily be eliminated by oxidation with O₂.

A large-scale, 7 lb./hr., preparation of dry N₂O₄ is planned. Equipment has been collected and assembly is nearly complete. Once

preliminary experience has been acquired, it should be feasible to generate sizeable quantities of dry N_2O_4 on a routine basis.

VI. Red Non-Reactive N_2O_4

In the context of this program, Red Non-Reactive N_2O_4 (RNR) is defined as material that is visually indistinguishable from RR N_2O_4 at $0^\circ C$. and which does not cause stress corrosion cracking in the standard test. Previous work had indicated that it was possible to have a sample that was visually "red" but which contained significant amounts of NO. Subjective visual assessments of color are influenced by the temperature dependence of the $N_2O_4 \rightleftharpoons 2 NO_2$ equilibrium, the depth of the solution observed, and basic red-green color sensitivity. A brief subjective test was set up to evaluate the above hypothesis.

Various proportions of prechilled RR and G8 N_2O_4 were mixed in 50 ml. glass-stoppered graduates and allowed to equilibrate in an ice bath. A series of four samples was prepared consisting of RR, 95RR:5G8, 90RR:10G8, G8. The mixtures were prepared by volume and the series corresponded to 0, 400, 800 and 8,000 ppm. NO. A panel of five individuals not associated with the program were called upon to view the samples individually. None of the panel could distinguish the 400 ppm. NO sample from RR N_2O_4 . Two of the five initially detected a greenish cast in the 800 ppm. sample. After having their attention focused on this sample, the other three panel members changed their minds and felt that they too could detect a hint of green color. The actual presence of NO in the 95:5 sample was confirmed by spectrophotometry.

At higher temperatures the greater equilibrium concentrations of NO_2 gives a darker red background and even larger amounts of NO could be present without imparting a perceptible green color to the N_2O_4 . These observations indicated that, based on visual examination at $0^\circ\text{C}.$, "red" N_2O_4 might contain 400-800 ppm. NO . This conclusion was substantiated when a sample of "red" N_2O_4 containing 500 ppm. of NO did not crack any of the alloy specimens in a standard SCC test.

VII. Future Work

Work in the final quarter of the contract period will center on the application of SCC tests to samples of dry N_2O_4 to which have been added various concentrations of NO , H_2O , and 100% HNO_3 . Experiments will also be conducted involving the adjustment of dissolved O_2 levels followed by SCC testing at temperatures below $60^\circ\text{C}.$ One or two experiments involving aqueous HNO_2 pretreatment will be repeated.

The main goals of this final phase of the work will be to clarify, as far as possible, the roles of O_2 and N_2O_3 in the creation and inhibition of stress corrosion cracking.

References

- (1) Coon, E. D., et al., U.S. Dept. Com., Office Tech. Serv., AD 220,479 (1959); C.A. 58 75976 (1963).
- (2) Chang, C. T. and N. A. Gokcen, J. Phys. Chem. 70, 2394 (1966).

Table 1

Stress Corrosion Cracking Tests, 6Al 4V ELI Ti Versus N_2O_4

Stress Cracking Run No.	N_2O_4 Type	Failure		Corrosion Rate, Mils/Yr.	Time, Hours	Temp. °C.	Test Conditions		Change from Basic N_2O_4 Comp.	O ₂ Content, ppm.	
		Rate	Description				Bend Orientation (Relative to Rolling Direction)	Stress, %, of Yield Strength		Before Test	After Test
4	RR	10/10	U-bends intact, many cracks	0.9 ^{+0.3} _{-0.2}	24	162	Parallel	90	None	-	-
5	G8	0/10	No cracks	Not detected <0.06	70	166	Transverse	90	None	-	-
6	RR	4/4 4/4 2/2	U-bends intact U-bends intact Cracks, perimeter band 1/16" in from edges of sheared, flat blanks.	0.8 ^{+0.1} 0.9 ^{+0.0}	69.2	165	4 Parallel 4 Transverse 2 Sheared Blanks No bend	{ Residual Bending, All specimens Free.	None	-	-
7	G4(3)	0/10	No cracks	Not detected (<0.06)	69	165	5 Parallel 5 Transverse	90	4,000 ppm. NO added.	-	-
8	RNR(3)	0/10	No cracks	0.14 ^{+0.09} _{-0.05}	70	165	5 Parallel 5 Transverse	90	500 ppm. NO added.	-	0.3
9	RR	10/10	2 of U-bend, numerous cracks including stamped area	-	64	167	5 Parallel 5 Transverse	90	None	5.5	0.2
10	RR	10/10	Limited number of cracks - 2 to 8/cm. ² , no cracks at stampings. U-bends intact.	Not detected (<0.06)	76	70-80	Parallel	90	Deoxygenated	1.1	1.3
11	RR	10/10	Large number of cracks - 100 to 800/cm. ² . U-bends intact.	-	76	70-80	5 Parallel 5 Transverse	90	None	20.1	19.1
12	RR	10/10	2 of U-bend, numerous cracks including stampings.	-	60	167	5 Parallel 5 Transverse	90	Deoxygenated	0.08	0.05
13	RR	10/10	Same as 12. Specimens pre-exposed to HNO ₂	-	67	163	5 Parallel 5 Transverse	90	None	-	-
14	RR+G8	5/5	Same as 12.	-	67	163	Parallel	90	Small amounts of G8 N_2O_4 added to reduce O ₂ level.	0.1	0.4

- (1) RR and G8 N_2O_4 each contain about 16 ppm. Cl.
No changes in Cl content have been detected in
4 SCC runs.
- (2) "Water" is present between 800 and 900 ppm. in
RR, G8, G4, and RNR N_2O_4 .
- (3) G4 and RNR N_2O_4 were made by equilibrating known
quantities of RR and G8 materials. Adjustments
of the mixtures to the desired NO level were made
with G8 N_2O_4 .

Table 2

Contamination of N₂O₄ by Metals During SCC Experiments

N ₂ O ₄ Type	Sample Source	Metal Concentration, ppm. (1)					Stress Corrosion Cracking
		Fe	Ti	Al	V	Na	
RR	Storage Cylinder	0.33	<0.8	<0.4	<0.1	-	-
	Corrosion Test Cell						
	Normal RR	0.3-0.9	26	0.4	9.0	-	Yes
	Deoxygenated RR via NO Add(3)	0.4	10	0.6	2.2	-	Yes
	Normal RR, HNO ₂ treated specimens	0.3	37	0.9	6.9	-	Yes
	Deoxygenated RR via degassing						
	Solution	0.3	10	<0.2	4.5	0.06	Yes
	Solution + Solids(2)	0.3-0.8	10-22	0.2-0.8	4.5	0.06-0.9	
G8	Storage Cylinder	1.1	<0.6	<0.3	<0.1	<1	-
(7,200 ppm. NO)	Corrosion Test Cell	1.6	<0.6	<0.3	<0.1	<1	No
500 ppm. NO(4)	Preparation Vessel	0.3	<0.8	<0.4	<0.1	-	-
	Corrosion Test Vessel	0.5	<0.8	<0.4	<0.1	-	No

(1) Analysis Method - Atomic Absorption.

(2) The solid residue amounted to about 100 mg. It analyzed 0.5% Fe, 13.3% Ti, 0.75% Al, <0.25% V, and 0.1% Na. "Solution + solids" values are based on the actual analysis of the liquid N₂O₄ corrected for the metals present in the solid residue.

(3) Only 5 U-bends used in this test. surface area is about 1/2 the normal value.

(4) This material made from G8 and RR N₂O₄.

Phase B. Characterization of Propellant N₂O₄

I. Determination of Oxygen by Gas Chromatography

A. Introduction

During the past quarter, a workable procedure has been developed for the gas chromatographic determination of dissolved oxygen in N₂O₄. Instrumental problems and problems of low recovery of dissolved oxygen from solvents have been overcome.

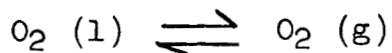
B. Discussion of Results

In order to circumvent equipment problems described in the last quarterly report, the previously used thermistor detector was discarded in favor of a hot-wire thermal conductivity cell. The latter detector is inherently more stable and rugged. To attain equivalent sensitivity, the detector is operated at a filament current of 350 milliamperes.

The liquid and gas sampling valves were also removed from the apparatus as a new sampling procedure was developed. Basic to the new procedure is the use of a glove bag which can be flushed to eliminate oxygen. Also necessary is the use of the new "Pressure Lok" gas syringe which allows a gas sample to be isolated in the syringe barrel under a maximum pressure of 250 psi.

The use of the glove bag and the advent of the new gas syringe suggested that analysis of the gas phase over N₂O₄ might be used as an indirect procedure for determining the concentration

of oxygen in the liquid phase. Such a method is attractive since the equilibrium



should, at room temperature, be highly shifted in favor of the gas phase. Thus, the oxygen peak should be large and, therefore, easily measured. Because of this, extrapolation to a concentration in the liquid phase should yield a sensitivity for oxygen in the liquid phase of well below 1 ppm. It has, in fact, been shown that a peak of 1 cm.² derived from oxygen in the gas phase calculates as 46 ppb. The limit of detection is probably close to 10 ppb., using a 2.0 ml. sample of the gas.

Sampling of the gas phase is much simpler than sampling the liquid N₂O₄. Since the boiling point is below room temperature, any liquid sampling device must be cooled or degassing of the N₂O₄ will occur. Examination of the gas phase also eliminates frequent cold trap venting since no water should be transferred to the system and the trap should plug infrequently as the amount of N₂O₄ introduced is small.

The use of a syringe to sample the liquid or gas is, however, preferred over either the liquid or the gas sampling valves. The syringe is easily cooled to eliminate degassing, the volume withdrawn from the bulk of the sample is small so that gas-liquid equilibria are not significantly changed, and the sample size can be varied.

Relation of the gas phase analysis to the concentration of oxygen in the liquid phase would not be possible were it not for the publication of values for the Henry's Law constant for oxygen in N_2O_4 (1). Thus, by determining the partial pressure of oxygen over N_2O_4 , the concentration can be calculated. The partial pressure of oxygen, P_{O_2} , in atmospheres is calculated from the gas laws by

$$P_{O_2} V = n RT = \frac{g RT}{M} \quad (1)$$

where R = the gas constant = 0.0821 l-atm./°K-mole

T = Absolute Temperature, °Kelvin

g = Weight of oxygen in grams

M = Molecular weight of oxygen = 32

V = Volume of the gas space in liters

now

$$g = \frac{F \times A_{O_2} \times 10^{-6} \text{ g./}\mu\text{g} \times V}{V'} \quad (2)$$

where F = the oxygen response factor in micrograms/cm.²

A_{O_2} = the area of the oxygen peak in cm.²

V' = the aliquot size in liters

substitution of equation (2) in (1) yields

$$P_{O_2} = \frac{F \times A_{O_2} \times R \times T \times 10^{-6}}{M \times V'} \text{ (atm.)} \quad (3)$$

From the relation (1),

$$X = K \times P_{O_2} \quad (4)$$

where X = mole fraction of oxygen in the liquid

K = reciprocal Henry's Law constant = 1.0168×10^{-3}

the ppm. O_2 in the liquid is given by,

$$\begin{aligned} \text{ppm. } O_2 &= 1.0168 \times 10^{-3} \times \frac{32 \text{ g. } O_2/\text{mole } O_2}{92 \text{ g. } N_2O_4/\text{mole } O_2} \times 10^6 \frac{\mu\text{g}}{\text{g.}} \times P_{O_2} \\ \text{ppm. } O_2 &= 353.66 \times P_{O_2} \end{aligned} \quad (5)$$

If the liquid N_2O_4 is analyzed directly, the concentration of oxygen is calculated from the relation

$$\text{ppm. } O_2 = \frac{F \times A_{O_2}}{d_{N_2O_4} \times V^T} \quad (6)$$

where $d_{N_2O_4}$ is the density of the N_2O_4 and is calculated from the relation $d_{N_2O_4} = 1.4916 - 0.00226 (t^\circ\text{C.})$ (1).

The experimentally found relationship between gas and liquid phase analyses is depicted by Figure 1; the data are given in Table 3. At high oxygen concentrations (>10 ppm.), the correspondence between gas and liquid analysis appears to be 1:1 or Curve A in Figure 1 is approached. In the 2 to 7 ppm. range, however, there is nearly a factor of two difference between the calculated (equations 3 and 5) and liquid phase (equation 6) results. The reason for discrepancy in the low range has not, as yet, been determined. It is most likely due to the inability

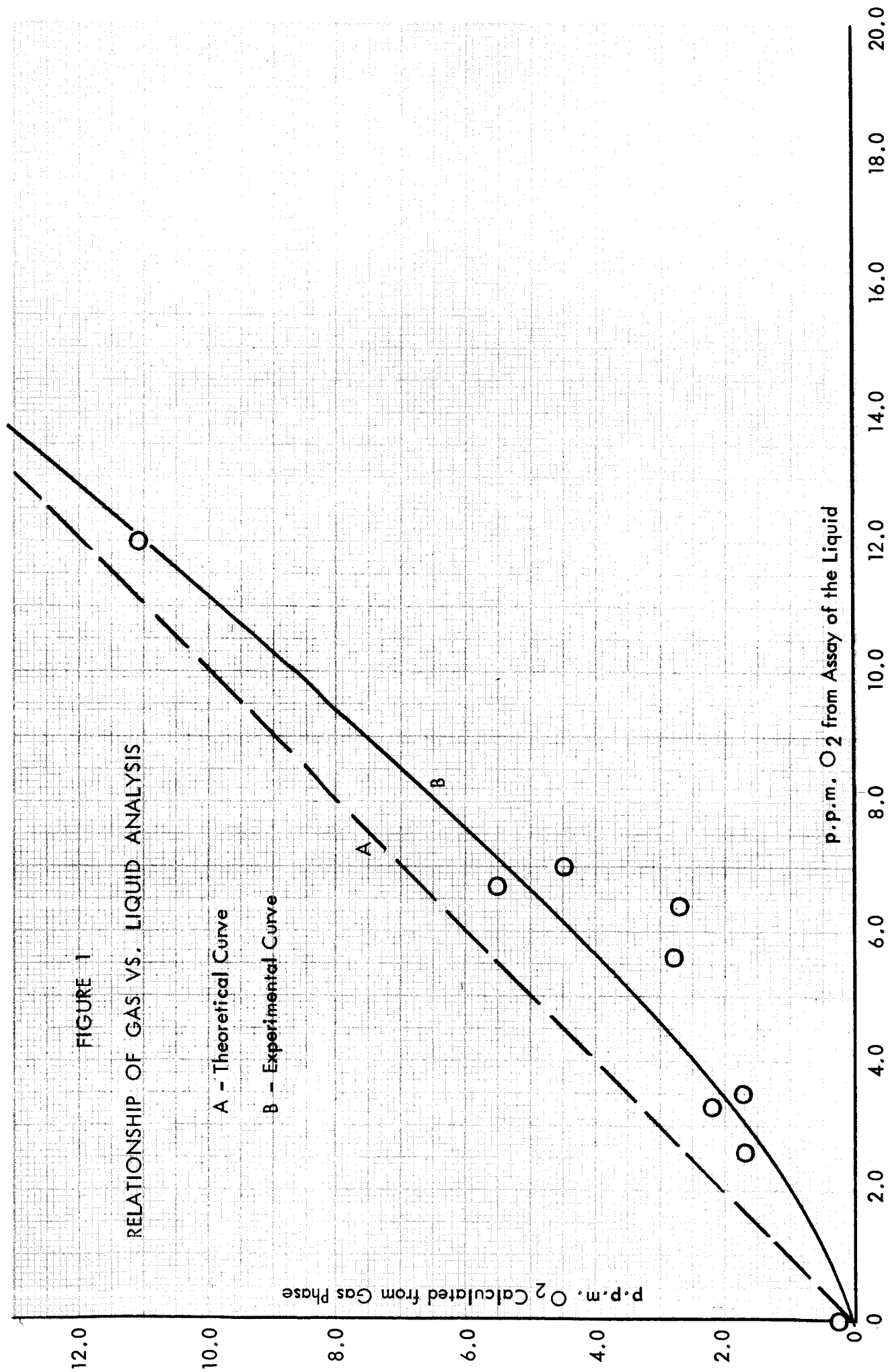


Table 3

Relationship of Gas Phase Analysis to Liquid Analysis

Designation	Partial Pressure of Oxygen in the Gas Phase (atm.) (a)	ppm. Oxygen in the Liquid Calc. from PO_2 in Gas (b)	No. of Detns.	s	% s	ppm. Oxygen in the Liquid by Direct Analysis (c)	No. of Detns.	s	% s
X15462-96-1	0.0315	11.1	5	0.0016	5.1	12.0	5	1.12	9.3
X16300-12A	0.0155	5.5	6	0.0018	11.6	6.7	5	1.0	14.9
-12B	6.87×10^{-4}	0.24	4	0.46×10^{-4}	6.6	Not Detected	4	-	-
X16300-28A	7.68×10^{-3}	2.7	4	0.72×10^{-3}	9.4	6.4	3	0.76	11.9
X16300-29A	4.89×10^{-3}	1.7	4	0.61×10^{-3}	12.4	3.5	3	0.07	2.0
X16300-30A	4.88×10^{-3}	1.7	4	0.83×10^{-3}	17.0	2.6	4	0.35	13.4
X16300-31A	0.0127	4.5	4	0.0011	8.7	7.0	3	0.59	8.4
X16300-34A	7.71×10^{-3}	2.7	5	0.40×10^{-3}	5.2	5.6	5	0.46	8.2
X16300-35A	0.1755	62.1	5	0.0060	3.4	61.5	7	3.15	5.1
X16300-36	6.22×10^{-3}	2.2	5	0.34×10^{-3}	5.5	3.3	5	0.39	11.8

(a) Calculated from Equation 3

(b) Calculated from Equation 5

(c) Calculated from Equation 6

to accurately calibrate at low oxygen levels. There is a definite discontinuity in the calibration data (see Table 5), the reason for which may only be due to measurement (sampling or area) errors. This will be further investigated, and until the reason is established an extrapolated value of F of 0.347 micrograms/cm.² will be used.

The developed method was also used to monitor the stress corrosion cracking (SCC) test cells for oxygen content during a study of the effect of oxygen on SCC. Included in this test series was a study of the degassing of oxygen from N_2O_4 by boiling off the N_2O_4 . The results of the various SCC tests are described under Phase A. The procedure has also been used to ascertain the oxygen content of various dry N_2O_4 samples used to calibrate for the ultraviolet NO method. These data along with SCC analytical results are summarized in Table 4.

C. Future Work

Work will continue on firming up the translation of gas phase results to concentrations of oxygen in the liquid phase. An investigation will be made into the calibration for oxygen at low levels.

Table 4

Summary of Analytical Oxygen Determinations

Designation	Po ₂ (Atm.)	Calculated O ₂ Level in Liquid (ppm.)	Direct Assay of Liquid (ppm.)	Sample Description
X15462-96-1 -2	0.0315 8.06 x 10 ⁻⁴	11.1 0.3	12.0 N.D.	RR-Mil-P-26539A G.5-500 ppm. NO
X16300-12A -12B	0.0155 6.87 x 10 ⁻⁴	5.5 0.2	6.7 N.D.	SCC Test - Run 9 RR SCC Test - Run 9 after heating
-16A	0.0340	12.0	-	SCC Test - Run 10 RR at R.T. before venting
-16B	3.65 x 10 ⁻³	1.3	-	SCC Test - Run 10 after venting and standing 76 hrs. - R.T.
-18A	0.0569	20.1	-	SCC Test - Run 11 - Room Temp.
-18B	0.0540	19.1	-	SCC Test - Run 11 - After 76 hrs.
-19A	7.13 x 10 ⁻³	2.5	-	SCC Test - Run 12 - Before heating
-19AV	2.43 x 10 ⁻⁴	0.08	-	SCC Test - Run 12 - After venting and before heating
-19AVH	1.39 x 10 ⁻⁴	0.05	-	SCC Test - Run 12 - After heating
-24	1.94 x 10 ⁻⁴	0.07	-	Dry N ₂ O ₄ + 240 ppm. NO
-27A	4.16 x 10 ⁻⁴	0.14	-	SCC Test - Run 14 - 100 ppm. NO before heating
-27B	1.07 x 10 ⁻³	0.37	-	SCC Test - Run 14 - After heating
-28A	7.68 x 10 ⁻³	2.7	6.4	} Dry N ₂ O ₄
-29A	4.89 x 10 ⁻³	1.7	3.5	
-30A	4.88 x 10 ⁻³	1.7	2.6	
-31A	0.0127	4.5	7.0	
-34A	7.71 x 10 ⁻³	2.7	5.6	
-35A	0.1755	62.1	61.5	
-36A	6.22 x 10 ⁻³	2.2	3.3	

D. Experimental Section

The overall apparatus used is essentially the same as described in the last quarterly report except that the liquid and gas sampling valves have been removed. The equipment presently used for sampling operations is shown in Figure 2. The apparatus is being used to routinely sample both the liquid and gas phases of standard sample bulbs and of the SCC test cells. A detailed description of sampling operations will be discussed in the final report under this project.

Suffice it to say that the oxygen level in the glove bag is reduced to $<0.1 \mu\text{g/ml}$. Although a much lower level is possible, the extent of sample contamination via a $0.1 \mu\text{g/ml}$ oxygen-in-helium atmosphere should be negligible.

1) Gas Chromatographic Conditions

Column: 12' x 1/4" O.D. SS packed with 52.9 grams of 13X molecular sieve and activated for 4 hrs. at 300°C .

Temperatures: Column, Injection Port, Detector all at ambient ($27 \pm 1^{\circ}\text{C}$.)

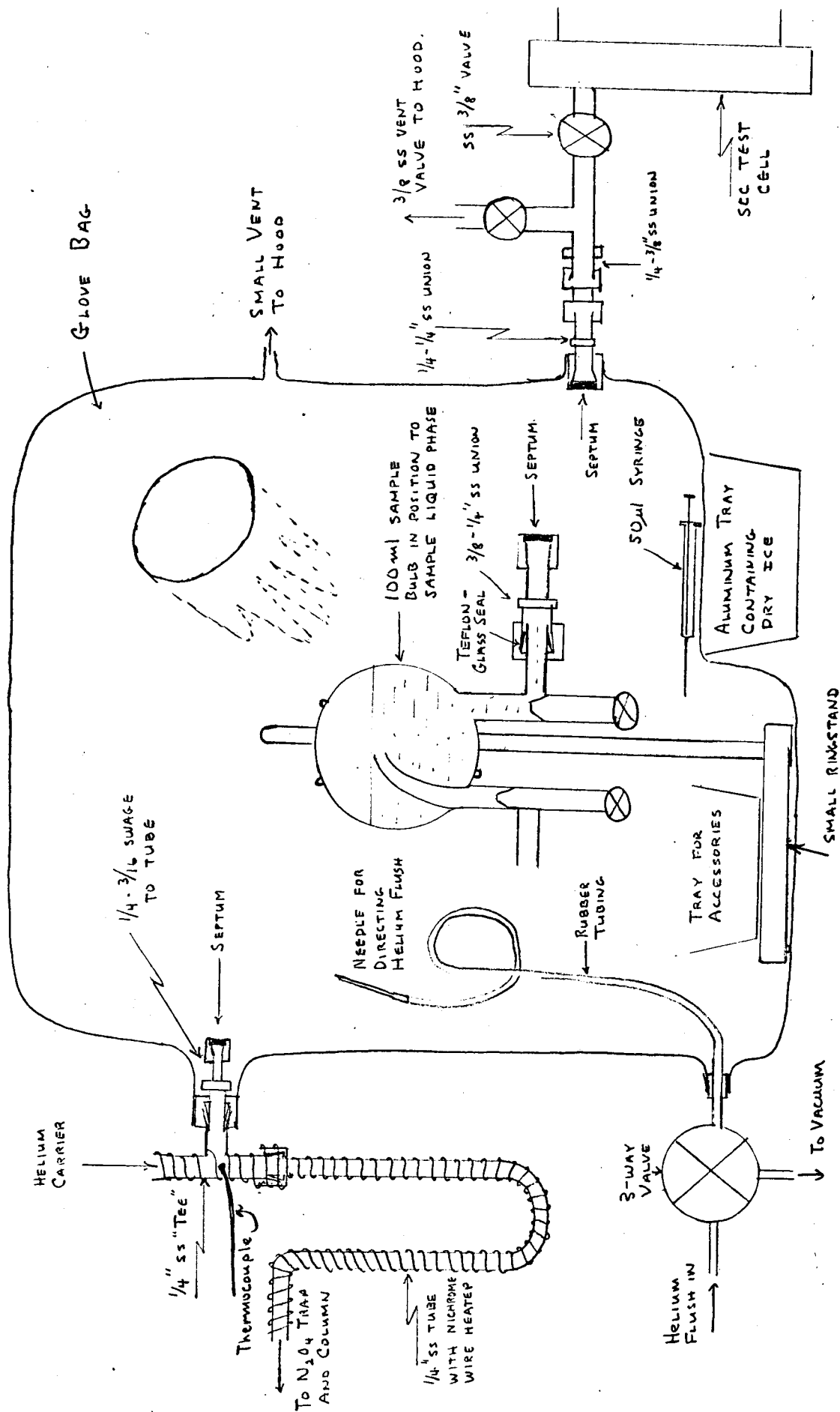
Carrier Gas: Helium at 40 ml./min.

Cold Trap: Dry ice - trichloroethylene (-78°C .)

Recorder: Brown, 1 mv., 1 sec. full scale

Detector: Hot-wire thermal conductivity cell at 350 milliamperes.

Figure 2
Gas Chromatographic Sampling System



2) Calibration

Calibration curves for oxygen (and nitrogen) were obtained by injecting various volumes of air into the chromatograph and determining the peak area in square centimeters by triangulation. The amount of oxygen injected into the gas chromatograph is calculated by rearrangement of equation 1 to

$$\text{g. O}_2 = \frac{M \times P \times V}{RT} \quad (7)$$

where V is now the volume, in microliters, of air injected.
and since air is 20 percent oxygen

$$\begin{aligned} \text{g. } (\mu\text{g}) \text{ O}_2 &= \frac{32 \times 1 \text{ atm.} \times \mu\text{l (air)} \times 0.2099}{0.0821 \times T^\circ\text{K}} \\ \mu\text{g O}_2 &= \mu\text{l (air)} \times 81.81/T^\circ\text{K} \end{aligned} \quad (8)$$

The response factor F is given by dividing the micrograms of oxygen injected by the area of the oxygen peak. This data from 0.3 to 108 micrograms of oxygen is given in Table 5. Above 0.8 micrograms of oxygen, a plot (Figure 3) of micrograms of oxygen versus peak area is linear over the entire range.

References

1. Chang, E. T. and Gokcen, N. A., J. Phys. Chem. 70, 2394 (1966).
2. Lange "Handbook of Chemistry", Handbook Publishers, Inc., Sandusky, Ohio, 1952.

Table 5
Calibration for Oxygen

Volume of Air Injected	Temp. °K	μg(a) Injected	Average Area (cm. ²)	Average F (μg/cm. ²)	No. of Detns.	S	% S
1.0	299.82	0.273	0.59	0.466	8	0.041	8.9
2.0	300.20	0.545	1.42	0.385	7	0.020	5.2
3.0	300.86	0.816	2.43	0.335	8	0.007	2.0
5.0	301.34	1.357	4.20	0.323	6	0.009	2.8
10.0	301.12	2.717	8.38	0.324	7	0.004	1.2
15.0	300.67	4.081	12.33	0.331	6	0.005	1.4
20.0	300.42	5.446	16.48	0.330	6	0.004	1.2
50.0	300.08	13.632	39.34	0.346	6	0.005	1.4
100.0	300.19	27.253	81.90	0.333	6	0.006	1.8
200.0	300.32	54.480	161.51	0.337	6	0.003	0.8
300.0	300.22	81.750	242.80	0.336	6	0.002	0.7
400.0	300.32	108.960	325.23	0.335	3	0.003	0.8
				$\bar{x} = 0.347$			

(a) Calculated from equation.

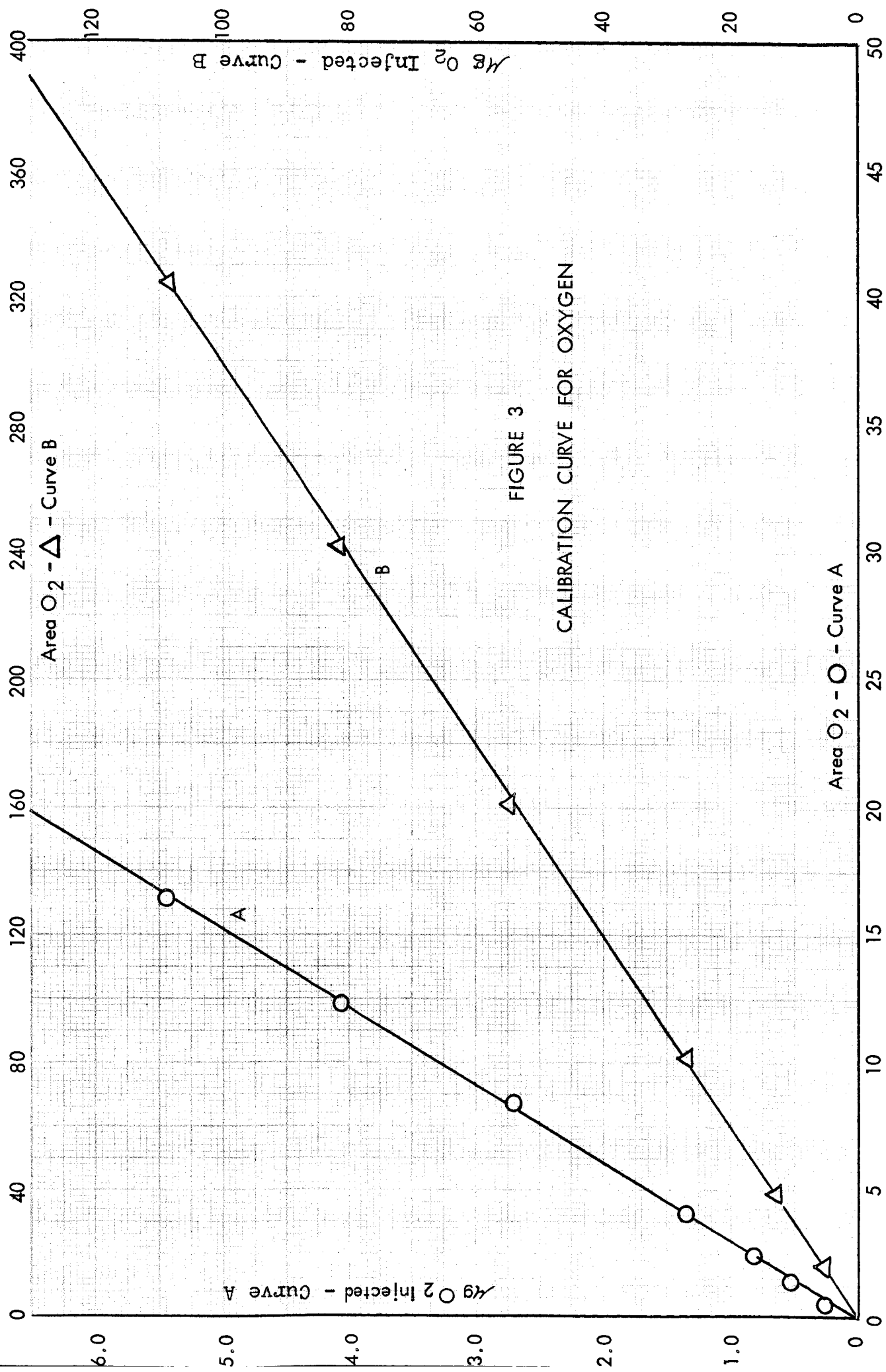


FIGURE 3
CALIBRATION CURVE FOR OXYGEN

II. Determination of NO by Visible Spectroscopy

The investigation of the limit of detection of NO as N_2O_3 was carried out simultaneously with an investigation of the effect of the concentration of protonated species in the sample on the shape of the absorption curve. In the second quarterly report, it was shown that below about 200 ppm. NO, the 700 μ maximum of N_2O_3 could no longer be observed, only a sloping, nondescript absorption was present. (See Curves A & B Fig. 4.) It was suspected that some different species was present at this low level which might be related to the protonated species concentration.

Several procedures were used in attempting to produce a "dry" N_2O_4 : (1) distillation of N_2O_4 from P_2O_5 , (2) distilling N_2O_4 and passing the vapor over P_2O_5 , (3) percolating liquid N_2O_4 through 3A mole sieve, (4) distilling N_2O_4 and passing the vapors over 3A mole sieve. Neither (1) or (2) produced N_2O_4 with "water" content below the NMR detection limit of 100 ppm. Both (3) and (4) produced "dry" N_2O_4 but generated NO in the process. Procedure (4) was adopted, followed by treatment with oxygen to eliminate NO, followed by degassing to remove excess oxygen. Reference samples were then prepared by adding 50, 100, 200, and 400 ppm. NO to dried, oxidized, degassed N_2O_4 and the spectra obtained at -10°C . in a 1 cm. cell (Fig. 4).

Even in the dry N_2O_4 the 700m μ maximum is not detected below 200 ppm. A differential spectrum was prepared by subtracting the spectrum of NO-free N_2O_4 (Curve O, Fig. 4) from the 50, 100, and 200 ppm. NO spectra (Curves A, B, and C, Fig. 4) and replotting. These differential spectra shown in Fig. 5 all show the 700m μ maximum. It can thus be concluded that there is no new species at low NO levels, but that the appearance of these spectra is due merely to the additive absorption of the N_2O_3 and the NO_2 background. The spectra do not appear to be affected by the presence or absence of protonated species.

The absorbance difference between 700 and 900m μ of these reference samples was plotted versus the amount of NO added (Fig. 6). Also plotted in this figure is a line representing the extrapolation of a measurement made at 4000 ppm. NO. The close similarity of the extrapolated and determined slopes indicate that the absorptivity is constant over this entire range. The comparison of added and found values in Table 6 demonstrates that little error probably accrues from using the extrapolated absorptivity value.

It is estimated that the limit of detection for NO in N_2O_4 will be about 15 ppm. While sufficient data for a good estimate of precision is not yet available, it would appear to be of the order of ± 15 ppm. at the less than 200 ppm. level.

Table 6 - Absorbance Versus NO Concentration

<u>ppm. NO Added</u>		<u>Measured Absorbance Difference 700-900mμ</u>	<u>ppm. NO found using absorptivity calculated at 4000 ppm. level</u>
<u>Uncorrected</u>	<u>Corrected*</u>		
0	0	0.0050 (Avg.)	0
63	51	0.0193	48
101	93	0.0318	89
200	195	0.0640	197
444	431	0.1288	413

* Corrected for O₂ content as determined by
gas chromatographic procedure prior to
addition of NO.

Figure 4

Absorption Spectra of N_2O_2 Dried by Distillation
through 3A Mole Sieve, O_2 treated, Degassed
to which has been added:

- | | |
|---|----------------|
| O | No NO |
| A | 51-63 ppm NO |
| B | 93-101 ppm NO |
| C | 195-200 ppm NO |
| D | 431-444 ppm NO |

Cary 14
MIR Source and Detector
1 cm Pathlength Cell
-10°C.

Absorbance

Wavelength in mμ

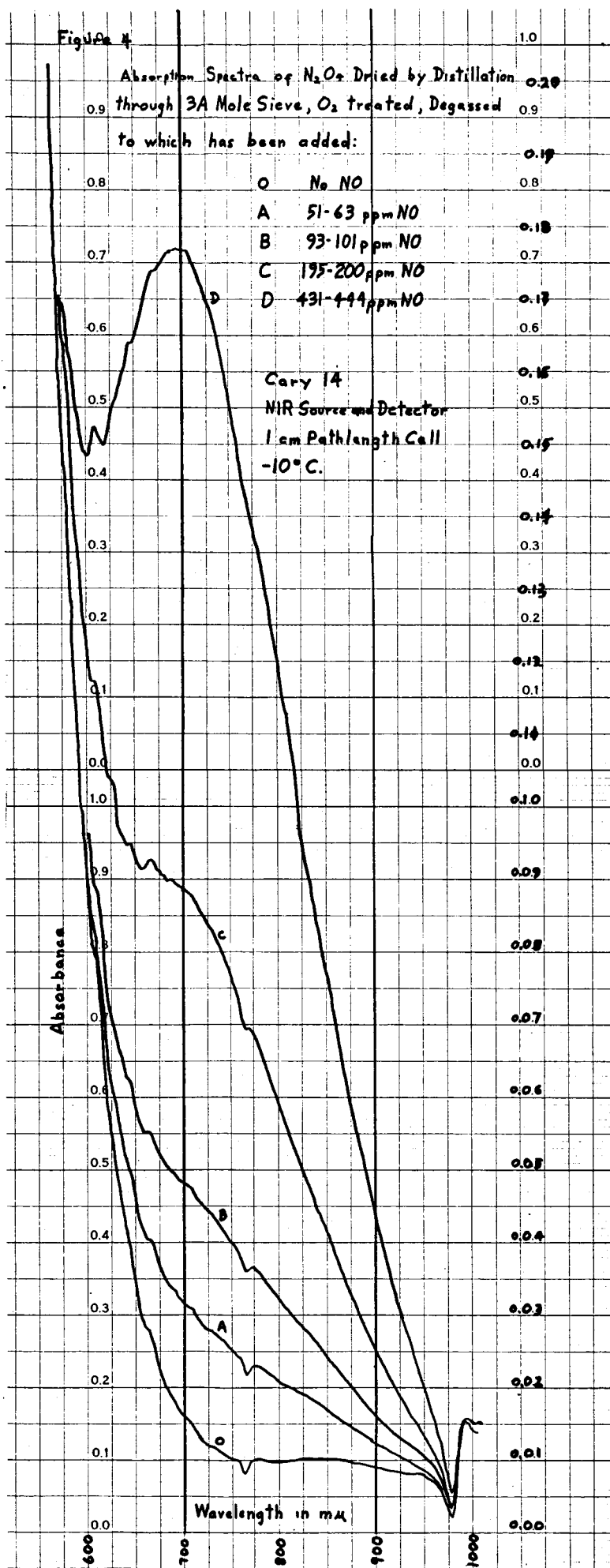


Figure 5

Replot of Spectra of Figure 4
from which the Contribution
of Curve 'O' has been Subtracted

Absorbance

Wavelength in $m\mu$

400

500

600

700

800

0.10

0.09

0.08

0.07

0.06

0.05

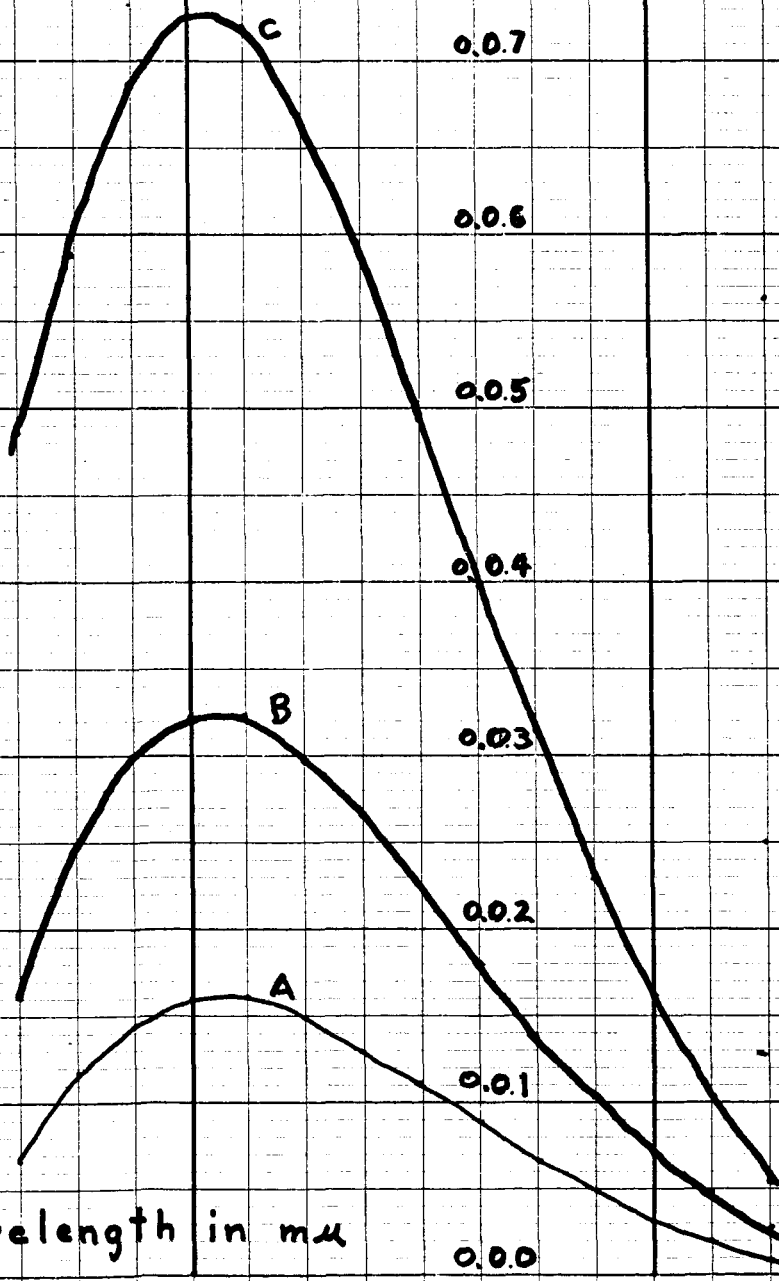
0.04

0.03

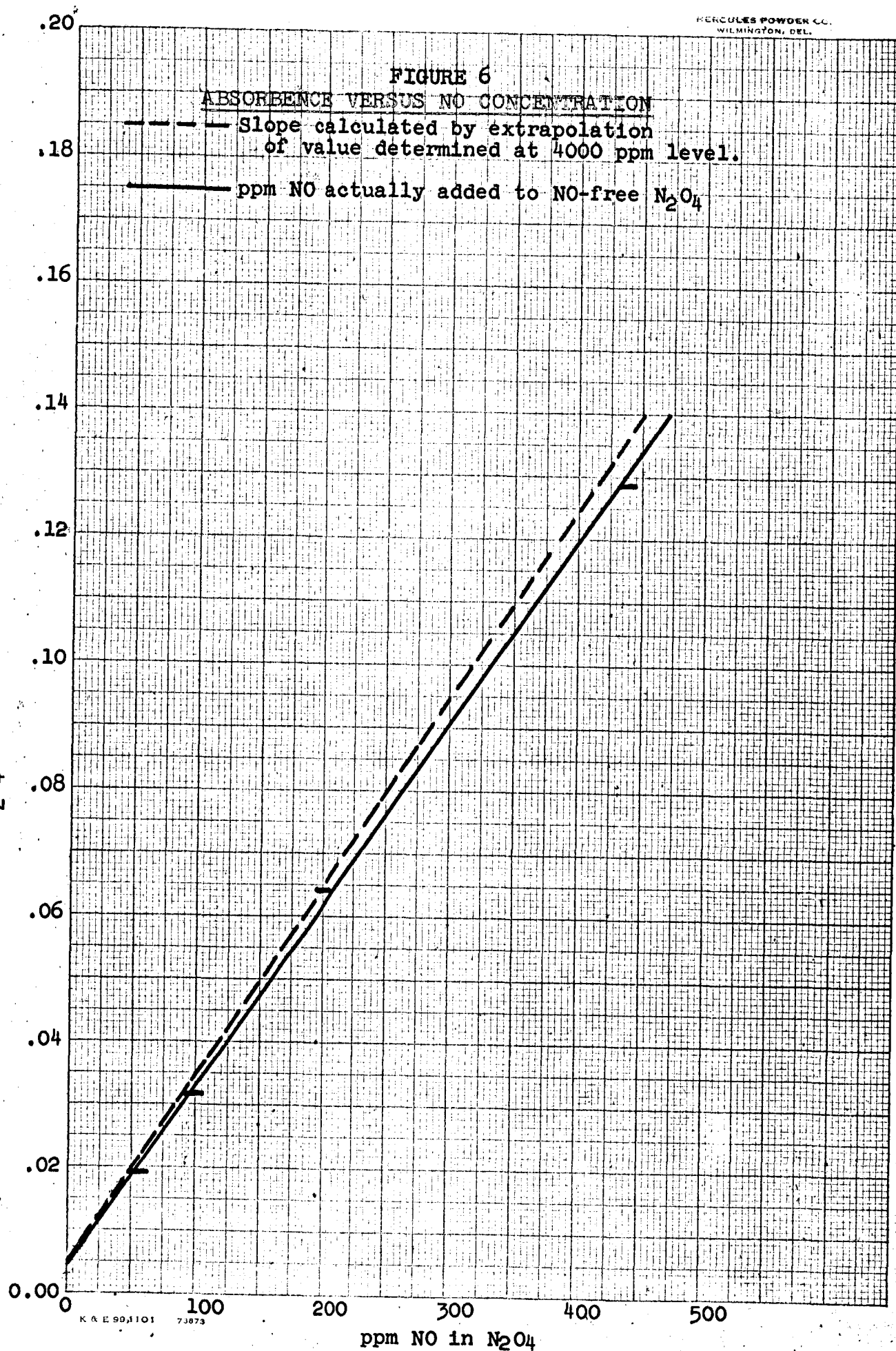
0.02

0.01

0.00



Absorbance difference between
700 and 900 millimicrons
of N_2O_4 in a 1 cm. cell at $-10^\circ C$.



III. The Determination of Dissolved Metals in N₂O₄

A. Introduction

The work during this period was aimed primarily at resolving discrepancies in the dissolved iron values obtained using different methods of analyses. In addition, continued monitoring of the Ti, Al, V and Fe contents of N₂O₄ samples, before and after exposure to titanium alloy, was provided during the period.

B. Discussion of Results

1. Resolution of Analytical Discrepancies

The major analytical discrepancy occurs between iron values obtained using a bathophenanthroline colorimetric extraction procedure and those obtained by other methods including atomic absorption spectroscopy, an orthophenanthroline colorimetric procedure (Hercules method M-100-38e) and another variation of a bathophenanthroline colorimetric procedure as described in a Rocketdyne Inc. Report (AFRPL-TR-67-277). The results of the latter three methods give soluble iron contents in the 0.5 to 1.6 ppm. range in contrast to the 5 to 15 ppm. found by the initial bathophenanthroline extraction procedure tried.

In addition to the varied finish procedures listed above, a number of sample preparation and concentration procedures were compared. These include open dish evaporation followed by

hydrolysis, water hydrolysis in a closed system with infrequent venting, followed by evaporation of the hydrolyzate, and hydrolysis in cold aqueous HCl in which the sample of N_2O_4 is slowly released below the surface of the hydrolyzing liquid to minimize escape of any possible volatile iron species before they are hydrolyzed. Finally, direct aspiration of N_2O_4 into the atomic absorption flame was accomplished. Tabulation of iron analysis results with various sample preparation and analytical finish combinations is given in Table 7. The results strongly indicate that the bathophenanthroline extraction procedure gives erroneously high results. Of particular relevance in coming to this conclusion are the low results obtained using the same hydrolysis and extraction but then changing the sample handling and finish to either atomic absorption or the Rocketdyne version of the bathophenanthroline procedure. Also of particular relevance are the low values obtained on direct aspiration and those obtained using large frozen samples taken directly from the storage tank and hydrolyzed under cold, closed conditions with minimal venting. These conditions should minimize or eliminate the loss of any significant quantities of volatile iron species. Since these values correspond well with those obtained under less stringent sample handling conditions, there does not appear to be any volatile iron in these samples.

2. Preferred Anal. Procedure

As a consequence of this investigation of analytical parameters, the general procedure that was adopted for service analyses combined the direct evaporation and subsequent water hydrolysis of the N_2O_4 sample with atomic absorption spectroscopy of the hydrolyzate. In this manner, the ease, speed, accuracy and sensitivity of atomic absorption is coupled with the most convenient and rapid sample concentration and hydrolysis technique, namely direct evaporation of N_2O_4 in a cold open platinum dish, followed by addition of water to the last 5 ml. of N_2O_4 . Very large N_2O_4 samples can be handled this way giving added sensitivity to the procedure.

3. Solubility of Ferric Nitrate

As a part of the above experiment program, attempts were made to dissolve $Fe(NO_3)_3$ directly in G-8 N_2O_4 for calibration of the atomic absorption spectrometer. The results were that less than 1 ppm. $Fe(NO_3)_3$ dissolved in G-8 N_2O_4 .

4. Visual Phenomena Noted During Evaporation of N_2O_4

N_2O_4 undergoes a number of visible changes during open dish evaporation. They are described here for the record. Typically, 125-150 g. are placed in a 200 ml. platinum dish which rests in an ice bath. When the sample volume has been reduced to approximately 5-10 ml., a distinct second liquid phase appears which then disappears upon further evaporation.

This may be an immiscible HNO_3 - N_2O_4 composition.

In addition, there occasionally is observed the formation of small clumps of yellowish cheesy solid after about half the N_2O_4 has evaporated. If lifted out of the liquid, the material decomposes or evaporates with evolution of reddish vapor. It is probably solid N_2O_4 formed locally by the rapid evaporative cooling.

5. Analysis of N_2O_4 Insolubles

The RRN_2O_4 from a SCC test run (No. 12) was found to leave an insoluble yellowish deposit on the walls of the glass sample flask after the latter had been emptied. Microscopically the residue was amorphous and gummy with the exception of small amounts of embedded birefringent crystals. An acetone-alcohol wash dissolved the amorphous phase leaving the crystals. The latter dissolved in concentrated HNO_3 . Estimating the total weight of material in both states as 10 mg., the atomic absorption analysis gives the following metallic composition of the combined residue:

0.5% Fe, <0.25% V, 13% Ti, 0.75% Al and 1% Na.

C. Experimental

The following are the pertinent experimental features of the various procedures investigated.

1. Bathophenanthroline Colorimetric Extraction Procedure

This method was obtained from the Hercules California plant and is the procedure used there for control analyses. The

liquid sample is weighed and sealed into glass ampoules, broken under the surface of dilute aqueous HCl and the N_2O_4 absorbed. Potassium sodium tartrate and hydroxylamine hydrochloride are added and the pH is adjusted to 4-5 with 8 N NaOH. The solution is transferred to a separatory funnel, bathophenanthroline reagent (0.001 M) is added and the Fe complex is extracted by shaking with isoamyl alcohol. The alcohol layer is filtered and transferred into a photometric cell and the absorbance at 533mμ read. Calibration is done using nitric acid solutions of Fe.

2. Rocketdyne Version of Bathophenanthroline Procedure (AFRPL-TR-67-277)

This is similar to above except that the bathophenanthroline reagent is 0.08%. Ammonium acetate and ammonium hydroxide buffer are used to adjust pH. The time of extraction and color development is specified at 10 min. and 15 min. respectively and the standards also contain HCl.

3. Orthophenanthroline Colorimetric Procedure (Hercules Method M100-38e)

The HCl solution of the sample is treated with orthophenanthroline reagent, made basic to Congo Red paper using NH_4OH-NH_4OAC buffer and after dilution to the mark the absorbancy is measured at 510mμ.

4. Atomic Absorption Spectroscopy

A Perkin-Elmer Model 303 Atomic Absorption Spectrophotometer was used.

5. Open Dish Evaporation and Hydrolysis

100-150 g. of cold N_2O_4 are placed in a 200 ml. platinum dish sitting in an ice bath. Evaporation down to about 5 ml. is followed by addition of 5 ml. H_2O . After hydrolysis, the volume is reduced nearly to dryness under low heat, brought up in a small amount of HNO_3 , and finally to volume with water.

6. Cold HCl Hydrolysis

Cold HCl (10%) is placed in an Erlenmeyer flask fitted with a ground glass stopper. The flask is placed in an ice bath. The precooled N_2O_4 sample (10 or 20 ml.) is drawn up in a pipet fitted with a stopcock and introduced very slowly beneath the HCl surface. The flask is loosely stoppered and allowed to come to room temperature. Alternately, the sample may be introduced either as a liquid in glass ampoule or as a frozen solid in an ampoule and broken under the surface.

Table 7 - Iron Content of N₂O₄

Sample	Analytical Prep Procedure	Analytical Finish Procedure	Results, ppm. Fe
G-8 Storage Tank	Evaporate, then hydrolyze Direct aspiration Cold HCl hydrolysis	Atomic absorption	0.93, 0.88, 0.79, 0.81, 0.73, 1.1
G-8 Storage Tank		Atomic absorption	0.68
G-8 Storage Tank		Atomic absorption	0.58, 0.78 Av. 0.81 S = 0.15
G-8 Storage Tank	Cold HCl hydrolysis	Orthophenanthroline colorimetric	0.67, 1.1 Av. 0.89 S = 0.30
G-8 Storage Tank	Bathophenanthroline Extractive Procedure		8.5
RR Storage Tank	Evaporate, then hydrolyze Direct aspiration Cold HCl hydrolysis	Atomic absorption	0.33, 0.32, 0.30, 0.31, 0.30, 0.33
RR Storage Tank		Atomic absorption	0.41
RR Storage Tank		Atomic absorption	0.36 Av. 0.33 S = 0.04
RR Storage Tank	HCl hydrolysis, extract into isoamyl alcohol As above with frozen samples	Bathophenanthroline (Rocketdyne Procedure)	0.34, 0.35 0.37, 0.35, 0.40 Av. 0.36 S = 0.02
RR Storage Tank	Bathophenanthroline Extractive Procedure		4.5, 4.7 Av. 4.6 S = 0.1
RR after SCC Test	Evaporate, then hydrolyze Closed H ₂ O hydrolysis Direct aspiration	Atomic absorption	1.3, 0.63, 0.97
RR after SCC Test		Atomic absorption	0.67, 0.97
RR after SCC Test		Atomic absorption	0.43 Av. 0.83 S = 0.3
RR after SCC Test	Evaporate, then hydrolyze Closed H ₂ O hydrolysis	Orthophenanthroline	0.80
RR after SCC Test		Orthophenanthroline	0.67 Av. 0.74 S = 0.1
G-8 after SCC Test	Evaporate, then hydrolyze	Atomic absorption	1.6

IV. Determination of Protonated Species by NMR

In the original proposal on which this contract was based, it was suggested that it might be possible to separate the proton peaks due to the acidic species in N_2O_4 by "freezing out" the equilibrium exchange process between the species. Since liquid N_2O_4 freezes at a relatively high temperature ($-10.2^\circ C.$), this cannot be done in pure N_2O_4 . For this reason, a study of the exchange process in solvent- N_2O_4 mixtures was begun in the last reporting period.

To date, solutions of RR N_2O_4 in $CHCl_3$ and CH_2Cl_2 have been examined (30-50 weight % N_2O_4) with no success. These solutions freeze in the -50 to $-60^\circ C.$ range, which is apparently not low enough to slow down the proton exchange to a point at which separate proton peaks are observed. A model system consisting of a 1:1 HNO_3 - H_2O mixture in acetone at the 1% level was run at $-80^\circ C.$ with no significant broadening of the acidic proton peak, so that it appears that an N_2O_4 -solvent mixture freezing below this temperature will have to be found.

The next step in the study will be to run the spectra of G8 N_2O_4 -solvent mixtures. In our previous analytical studies it was found that the line width of the acidic proton peak in N_2O_4 containing NO (as N_2O_3) is significantly greater than in RR N_2O_4 , and the line width increases with the amount of NO in the sample. We are not yet certain whether this represents a slowing of the exchange reaction, since the line width in green N_2O_4 does not appear to be measurably temperature dependent in the $+20^\circ C.$ to $-10^\circ C.$ range, but solvent- N_2O_4 mixtures will be studied at lower temperatures.